Acta Cryst. (1998). D**54**, 175–183

Structure of Balhimycin and its Complex with Solvent Molecules

MARTINA SCHÄFER,[a] GEORGE M. SHELDRICK,[a]* THOMAS R. SCHNEIDER[b]† AND LÁSZLÓ VÉRTESY[c]

[a]*Institut für Anorganische Chemie der Universität Göttingen, Tammannstrasse 4, D-37077 Göttingen, Germany,* [b]*European Molecular Biology Laboratory, c/o DESY, Notkestrasse 85, D-22603 Hamburg, Germany, and* [c]*Hoechst AG, D-65926 Frankfurt am Main, Germany. E-mail: gsheldr@shelx.uni-ac.gwdg.de*

(*Received 20 February 1997; accepted 13 June 1997*)

Abstract

Balhimycin is a naturally occurring glycopeptide antibiotic, related to vancomycin which acts by binding nascent bacterial cell-wall peptide ending in the sequence D-Ala-D-Ala. Crystals of balhimycin are monoclinic, space group $P2_1$, a = 20.48 (10), b = 43.93 (21), c = 27.76 (14) Å, β = 100.5 (5)° with four independent antibiotic molecules, three molecules of 2-methyl-2,4-pentanediol, two citrate ions, three acetate ions and 127.5 water molecules in the asymmetric unit. With an asymmetric unit larger than those of the smallest proteins and a solvent content of about 32%, the crystals have similar diffraction properties to those of small proteins. 27 387 unique reflections were collected using synchrotron radiation. The structure was solved by a standard protein technique, the molecular-replacement method, using ureido-balhimycin as search model. The anisotropic refinement against all F^2 data between 0.96 and 45 Å converged to a conventional R value of 11.27% with $R1 = \sum ||F_o| - |F_c|| / \sum |F_o|$ for the 24 623 data with $I > 2\sigma(I)$ and 12.58% for all 27 387 data. The four monomers possess fairly similar conformations (r.m.s. deviation 0.7 Å). Two antibiotic molecules form a tight dimer with antiparallel hydrogen bonds between the peptide backbone as well as between the vancosamine residues and the peptide backbone. In each of the two dimers, one binding pocket is occupied by a citrate ion and the other by an acetate ion. The dimer units are linked in the crystal by hydrogen bonds to form infinite chains.

1. Introduction

Balhimycin is a member of the vancomycin group of glycopeptide antibiotics (Nadkarni *et al.*, 1994; Chatterjee *et al.*, 1994). The best known glycopeptide antibiotic is vancomycin, isolated from *Nocardia orientalis*, first reported in 1956 (Levine, 1987; Cunha, 1995; Barna & Williams, 1984; Reynolds, 1989). Since then vancomycin has played an important role in the treatment of *C. difficile* diarrhoea or Gram-positive coccal infections in hemodialysis patients. Because of various side effects like the 'red man syndrome' and the necessity of intravenous administration of vancomycin, it was only used as a last resort (Polk *et al.*, 1993). Since the 1980's, when methicillin-resistant *S. aureus* (MRSA) became a major problem worldwide, the use of vancomycin has increased.

Vancomycin and other glycopeptide antibiotics have a common mode of action. They complex the C-terminal D-Ala-D-Ala peptides of the bacteria cell wall, preventing their cross linking. Many NMR studies, in particular by Williams and coworkers, showed that vancomycin and almost all other glycopeptide antibiotics form dimers in solution. They also deduced the hydrogen-bonding pattern for the interaction with the L-Lys-D-Ala-D-Ala peptide sequence (Waitho & Williams, 1989; Gerhard *et al.*, 1993; Groves *et al.*, 1994; MacKay *et al.*, 1994; Pearce & Williams, 1995; Pearce *et al.*, 1995; Beauregard *et al.*, 1995; Prowse *et al.*, 1995). Nevertheless, more crystallographic structural details of the antibiotic molecules themselves and their complexes with analogues of cell-wall peptides are urgently needed. This could provide ideas for modifying the antibiotic molecules to gain time in the struggle against bacterial resistance (Brant *et al.*, 1994; Neu, 1992; Arthur & Courvalin, 1993; Walsh, 1993; Walsh *et al.*, 1996).

The first crystal structure of a close relative of vancomycin was that of its degradation product CDP-1 (Sheldrick *et al.*, 1978). Subsequent NMR studies (Harris *et al.*, 1983) showed that the amide hydrolysis also caused an unexpected ring rearrangement which may have prevented dimerization; at the time a stroke of luck because otherwise the structure would have been too large to have been solved using conventional 'small-molecule' direct methods. Many years passed before the next X-ray structures of naturally occurring glycopeptide antibiotics were determined (Sheldrick *et al.*, 1995; Schäfer, Pohl *et al.*, 1996; Schäfer, Schneider *et al.*, 1996; Loll *et al.*, 1997). It was difficult to obtain suitable single crystals which diffract to atomic resolution (say better than 1.2 Å) and conventional direct methods were not capable of solving structures of such unsymmetrical dimers with more than 200 non-H atoms in the asymmetric unit. With the advent of powerful synchrotron radiation sources, the wide acceptance of cryogenic techniques, and the enormous increases in available

† Present address: Institut für Anorganische Chemie der Universität Göttingen, Germany.

computer power, new developments in *ab initio* structure solution became possible. The first published crystal structure of a true glycopeptide antibiotic, ureido-balhimycin (Sheldrick *et al.*, 1995) was solved using a new automated Patterson interpretation technique. The second one, an aglycone of ristocetin, was solved by an iterative combination of tangent formula phase expansion in reciprocal space and 'peaklist optimization' in real space (Schäfer, Pohl *et al.*, 1996; Sheldrick & Gould, 1995). Last but not least, the crystal structure of vancomycin itself was recently solved by two independent groups (Schäfer, Schneider *et al.*, 1996; Loll *et al.*, 1997) using new real/reciprocal-space recycling techniques (Miller *et al.*, 1993, 1994; Sheldrick & Gould, 1995). In the vancomycin structure, one postulated binding pocket of the dimer is occupied by an acetate ion, whereas the remaining one is closed by the asparagine side chain. It is believed that *in vivo* the vancomycin dimer inserts itself between the different glycopetide strands as shown schematically in Fig. 1.

Balhimycin was isolated from the fermentation broth of an *Amycolatopis* sp. Y-86,21022 (Nadkarni *et al.*, 1994; Chatterjee *et al.*, 1994). It belongs to the vancomycin class of the glycopeptides and contains a dehydrovancosamine sugar (Fig. 2). The *in vitro* and *in vivo* activity of balhimycin against MRSA strains is comparable to vancomycin; against anaerobes, particularly *Clostridium* strains, balhimycin showed superior bactericidal activity to that of vancomycin. Balhimycin possesses a hydrated ketosugar (Nadkarni *et al.*, 1994; Vértesy *et al.*, 1996) that makes it readily amenable to structural modification. The toxicity of balhimycin is comparable to that of vancomycin.

Crystals were obtained in the monoclinic space group $P2_1$ and a high-resolution data set was collected using synchrotron radiation. With unit-cell dimensions larger than those of small proteins like rubredoxin or crambin, around 400 peptide atoms and 32% solvent content this structure seemed to be a good candidate to test new *ab initio* methods. Alternatively molecular replacement could be employed using the ureido-balhimycin structure (Sheldrick *et al.*, 1995) as search model. The region of the postulated binding pocket, which was filled with water in the ureido derivate, was also of considerable interest.

2. Experimental

2.1. *Crystallization of balhimycin*

Preliminary crystallization attempts showed that the presence of citrate reduced the solubility of the antibiotic and appeared to favour crystal growth. Single crystals of balhimycin (Fig. 3) were obtained at 277 K by vapour diffusion using either the hanging-drop or sitting-drop method. Balhimycin drops were equilibrated against reservoir solution containing 10 m*M* HEPES buffer at pH 7.0, 10 m*M* sodium citrate and 25%(*v*/*v*) 2-methyl-2,4-pentanediol. The drops consisted of balhimycin-acetate at a concentration of 40 mg ml^{-1} in 10 m*M* HEPES buffer at pH 7.0 diluted with an equal volume of reservoir solution. Thin plates appeared after 2 d.

2.2. *X-ray data collection*

To avoid radiation damage, data were collected from a single crystal at 100 K. Therefore, the crystal (0.2 × 0.2

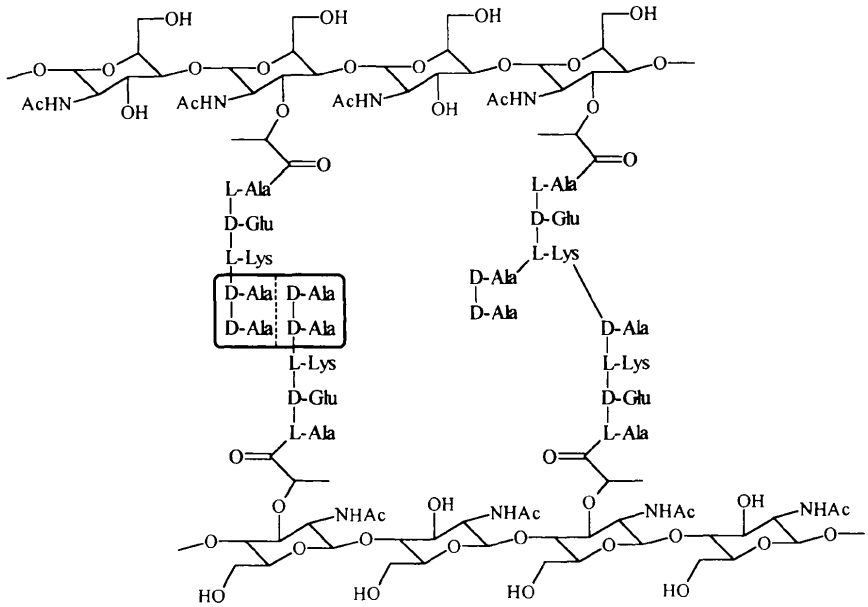

Fig. 1. Proposed insertion of vancomycin molecule between two different peptidoglycan strands. The two halves of the box represent the two monomers.

× 0.05 mm) was mounted in a loop (Garman & Schneider, 1997; Rogers, 1994; Teng, 1990) made from unwound dental floss, and immediately flash cooled, without the addition of further cryoprotectant. Data were collected on beamline X11 at EMBL c/o DESY in Hamburg, using a wavelength of 0.927 Å. Data were collected in two passes with the same crystal at high and low resolution with different exposure times. High-resolution data were collected with a MAR Research image-plate scanner (300 mm) at a crystal-to-detector distance of 90 mm with a φ range of 178° and a φ increment of 1°. Low-resolution data were collected using the same MAR Research image-plate scanner (180 mm) at a crystal-to-detector distance of 230 mm with the same φ range as above but with a 3° φ increment. Data integration and merging were performed using the program system *HKL* (Otwinowski & Minor, 1996). No absorption or decay corrections were applied. Reflection data statistics are summarized in Table 1, crystal data are given in Table 2.

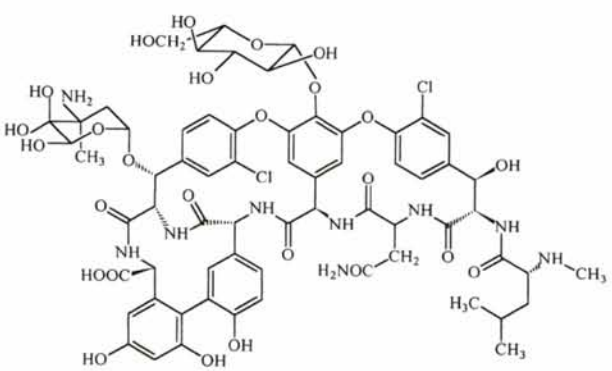

Fig. 2. Chemical formula for balhimycin.

Fig. 3. Picture of a single crystal of balhimycin. This crystal was grown by Dr Bob Cudney under similar conditions to those employed for the crystal used for data collection; we are grateful to him for providing this photograph.

2.3. *Structure solution*

The unit-cell volume of 24 542 Å^3 was consistent with four antibiotic molecules (each consists of 102 non-H atoms) in the asymmetric unit and a solvent content of about 32%. We expected to find two dimers related by non-crystallographic symmetry. Our first attempts to solve the structure using conventional direct methods failed, as did automated Patterson interpretation (Sheldrick, 1990; Sheldrick *et al.*, 1993) to locate the Cl atoms. Also with new real/reciprocal-space recycling techniques a structure solution has not been achieved yet. We were able to solve this structure using the molecular replacement method with the known ureido-balhimycin structure as search fragment and the program *AMoRe* (Navaza, 1994). Although we expected relatively high thermal motion for the glucose and vancosamine residues in balhimycin the whole ureido-balhimycin dimer was employed as search model. After the structure has been solved, the r.m.s. deviation of the ureido-balhimycin dimer to one balhimycin dimer was found to be 0.9 Å, which is higher than we had anticipated in view of their chemical similarity.

The rectangular *P*1 cell of 36 × 36 × 30 Å, used to calculate the Fourier transform of the model, was chosen approximately equal to the smallest box containing the model, plus the maximal distance of an atom from the center of mass, plus the resolution of the data (Navaza, 1994). The cross-rotation function was calculated within the resolution range 7–3.5 Å to find an initial orientation of the model. With correlation coefficients (Fujinaga & Read, 1987) of 0.299 and 0.296, respectively, the first two solutions were clearly separated from the next best solution with a correlation coefficient of 0.252. For the best ten rotation solutions the fast translation function was calculated for the resolution range of 7–3.5 Å. The first rotation solution again gave the highest correlation

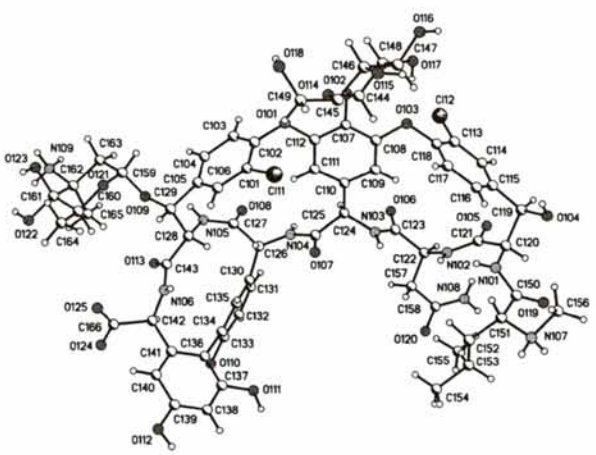

Fig. 4. Three-dimensional structure of one monomer of balhimycin with the numbering scheme. All other monomers have a similar numbering scheme.

coefficient of 0.25 and lowest R value of 62.3%, nevertheless this solution was not well seperated from the remaining noise peaks. We fixed this solution and calculated the fast translation function again with the remaining best rotation solutions to find the displacement of the expected second dimer. If the fixed solution for the first dimer has been assigned correctly, the improvement of the calculated phases should indicate clearly the position of the second dimer by a much higher correlation coefficient than for the other solutions. In

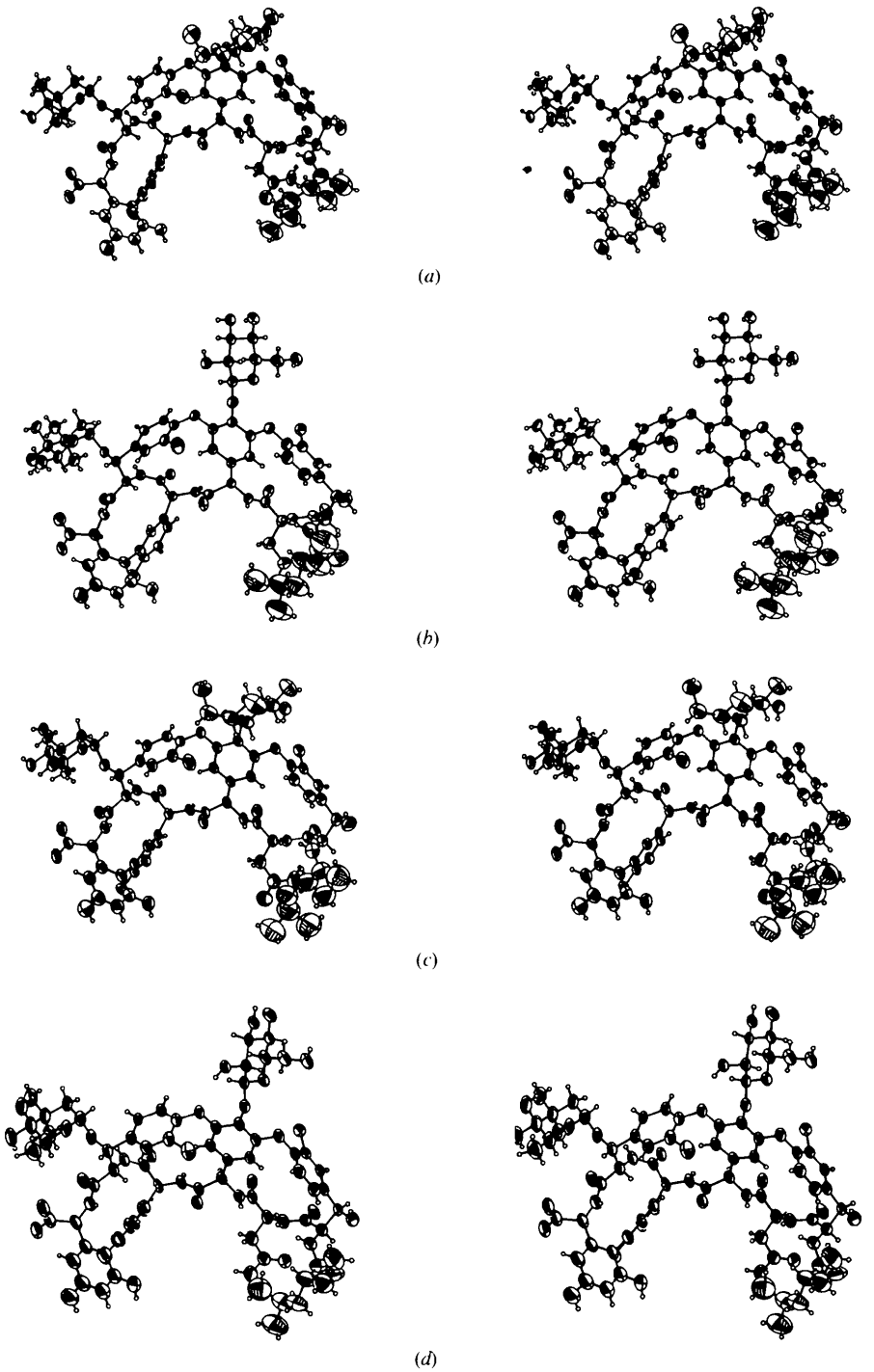

Fig. 5. (*a*)–(*d*) Stereoview of the 50% probability atomic displacement ellipsoids of the four independent monomers.

Table 1. *Reflection data statistics for balhimycin*

Range (Å)	Unique	% complete	% with $I > 2\sigma$	$R_{sym}(I)$ (%)†	R (%)	$R(I > 2\sigma)$ (%)
∞–2.65	1421	98.6	93.4	4.6	21.5	17.0
2.65–1.80	3006	96.6	95.9	4.5	12.0	11.9
1.80–1.45	3921	96.0	93.3	4.9	10.3	10.1
1.45–1.25	4529	94.2	89.4	6.1	10.1	9.7
1.25–1.10	5751	92.3	85.0	7.1	9.4	8.7
1.10–1.00	5809	90.0	74.8	10.4	10.7	8.8
1.00–0.96	2950	80.8	56.1	14.6	15.5	10.5
All data	27387	91.92	82.61	5.1	12.6	11.2

† $R_{sym}(I) = \sum |I - \langle I \rangle| / \sum |\langle I \rangle|$, where $\langle I \rangle$ is the mean intensity of a set of equivalent reflections. $R = \sum ||F_o| - |F_c|| / \sum |F_o|$ The percentage of unique reflections measured and the percentage with $I > 2\sigma(I)$ are both expressed in terms of the theoretical number of unique reflections.

this step the correlation coefficient for the second dimer was 0.43 compared with the highest noise peak of 0.29. For the R factors the difference between the correct solution and the best noise peak was much smaller (55.8 and 58.8%, respectively). As observed by Navaza & Vernoslova (1995) the correlation coefficient is a more sensitive indicator of the correct solution. Finally, we performed a fast rigid-body refinement of both dimers to minimize the errors in the positional parameters of the model. The rigid-body refinement is also useful for verifying the solution; the correlation coefficient should rise and the R factor should decrease, otherwise the solution could be wrong. In this case the correlation coefficient rose from 0.43 to 0.56 and the R factor dropped from 55.8 to 46.3%. The remaining atoms were located by difference Fourier syntheses in the course of refinement.

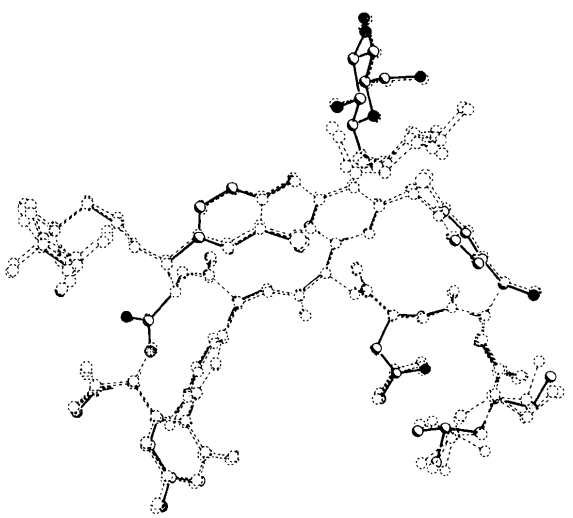

Fig. 6. Least-squares fit of all four monomers for all non-H atoms except all glucose residues.

Table 2. *Crystal data and structure refinement for balhimycin*

Empirical formula	$C_{66}H_{77}Cl_2N_9O_{25} + \frac{1}{2}C_6H_5O_7 + \frac{3}{4}C_6H_{14}O_2 + \frac{3}{4}C_2H_4O_2 + 31\frac{7}{8}H_2O$
Formula weight (g mol^{-1})	2288.7
Temperature (K)	100
Wavelength (Å)	0.927
Crystal system	Monoclinic
Space group	$P2_1$
Unit-cell dimensions (Å,°)	a = 20.48 (10) b = 43.93 (21) c = 27.76 (14) β = 111.50 (10)
Volume (Å^3)	24542 (212)
Z	8
Density (calculated) (Mg m^{-3})	1.239
Absorption coefficient (mm^{-1})	0.15
$F(000)$	9758
Crystal size (mm)	0.2 × 0.2 × 0.05
Reflections collected	103021
Independent reflections	27387 (R_{int} = 0.051)
Refinement method	Conjugate-gradient solution of least-squares normal equations
Data/restraints/parameter	27387/7307/5545
Goodness-of-fit S†	1.55
$g1$, $g2$‡	0.2, 0.0
Final R indices [$I > 2\sigma(I)$]‡§	$R1$ = 0.1127, $wR2$ = 0.2875
R indices (all data)‡§	$R1$ = 0.1258, $wR2$ = 0.3049
Absolute structure parameter	10 (10)
Max. difference density (e Å^{-3})	1.083
Min. difference density (e Å^{-3})	−0.923

† $S = \{\sum[W(F_o^2 - F_c^2)^2]/(n-p)\}^{1/2}$.
‡ $wR2 = \{\sum[w(F_o^2 - F_c^2)^2]/\sum[w(F_o^2)^2]\}^{1/2}$; $w^{-1} = s^2(F_o^2) + (g_1P)^2 + g_2P$, where $P = (F_o^2 + 2F_c^2)/3$.
§ $R1 = \sum ||F_o| - |F_c|| / \sum |F_o|$.

2.4. *Structure refinement*

The structure was refined against all F^2 values using the program *SHELXL* (Sheldrick & Schneider, 1997). All non-H atoms were refined anisotropically. The H atoms were included in calculated positions with idealized geometry and refined using a riding model. Chemically equivalent 1,2- and 1,3-distances in the four monomer units were restrained to be equal (with e.s.d.'s of 0.02 and 0.04 Å, respectively) but without imposing target values. Distance restraints (Engh & Huber, 1991; Rademacher, 1987) were applied to the citrate ions, the acetate ions and the 2-methyl-2,4-pentanediol molecule. Planarity restraints were applied to all aromatic systems and to all sp^2 hybridized C atoms (e.s.d. = 0.05). For anisotropic refinement 'hard' rigid-bond restraints (Rollet, 1970; Hirshfeld, 1976; Trueblood & Dunitz, 1983) were applied to the differences in mean-square displacement amplitudes along 1,2- and 1,3-distances (e.s.d. = 0.005 Å^2), and similarity restraints (e.s.d. 0.01 Å^2, or 0.1 Å^2 for terminal atoms) were applied to the corresponding U^{ij} components of atoms within 1.7 Å of each other. The solvent water molecules were restrained to be approximately isotropic with e.s.d.'s. of 0.1 Å^2. 'Anti-bumping' restraints were generated automatically to

prevent close contacts between isolated solvent molecules. All water molecules were refined as either fully occupied or half occupied. The refinement converged to a final $wR2 = 30.48\%$ with $wR2 = \{\sum[w(F_o^2 - F_c^2)^2] / \sum[w(F_o^2)^2]\}^{1/2}$ and $w^{-1} = \sigma^2(F_o^2) + (g_1P)^2 + g_2P$, where $P = (F_o^2 + 2F_c^2)/3$. The conventional $R1$ value ($R1 = \sum ||F_o| - |F_c|| / \sum |F_o|$) converged to 11.26% for the 24 623 data with $I > 2\sigma(I)$ and to 12.57% for all 27 387 data. The known absolute configuration was assumed throughout the refinement; the Flack x parameter (Flack, 1983; Bernardinelli & Flack, 1984) refined to 10 (10); in view of the short synchrotron wavelength, it is not surprising that this value does not provide a satisfactory enantiomorph discrimination.

The relatively high percentage of weak reflections at low resolution is associated with a pseudo-A lattice caused by the non-crystallographic symmetry; the mean intensity of the reflections with $(k + l)$ odd is about 50% of the overall mean intensity for $\infty > d > 5$ Å, but about 90% for the full resolution range. The unusual variation of $R1$ (and R_{sym}) with resolution may arise from a sampling error introduced by the high scan speeds used for the low-resolution frames, even though we attenuated the direct beam for these frames.

3. Results and discussion

The structure of balhimycin is shown in Fig. 2. Balhimycin crystallizes with four independent antibiotic

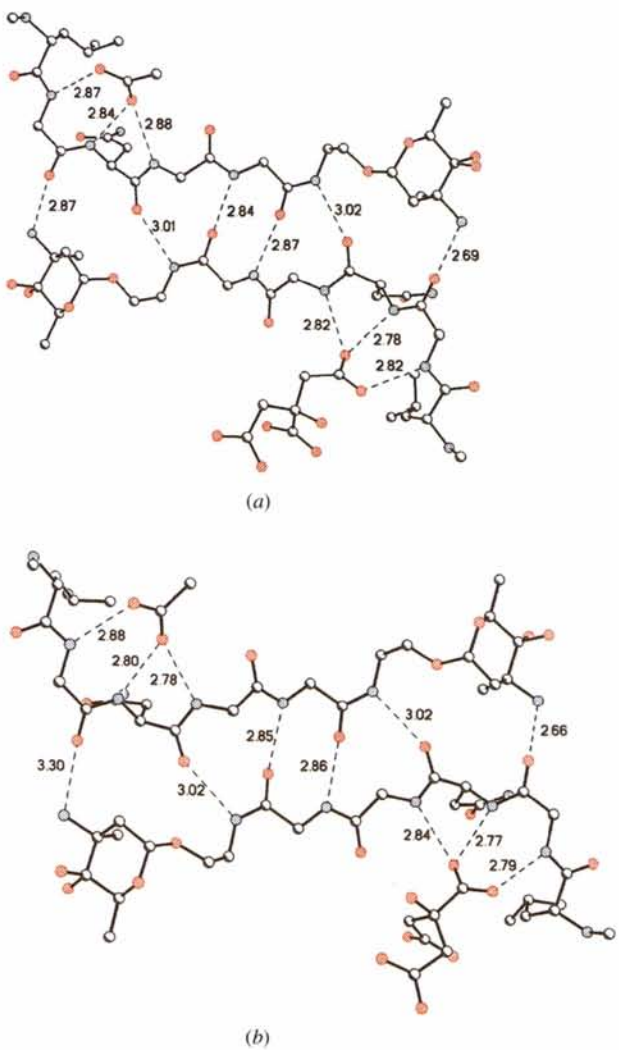

Fig. 7. The dimer interface and binding pocket of monomer (*a*) dimer *A* (monomers 1 and 2) and (*b*) dimer *B* (monomers 3 and 4). The hydrogen bond between the glucose residues is omitted for clarity.

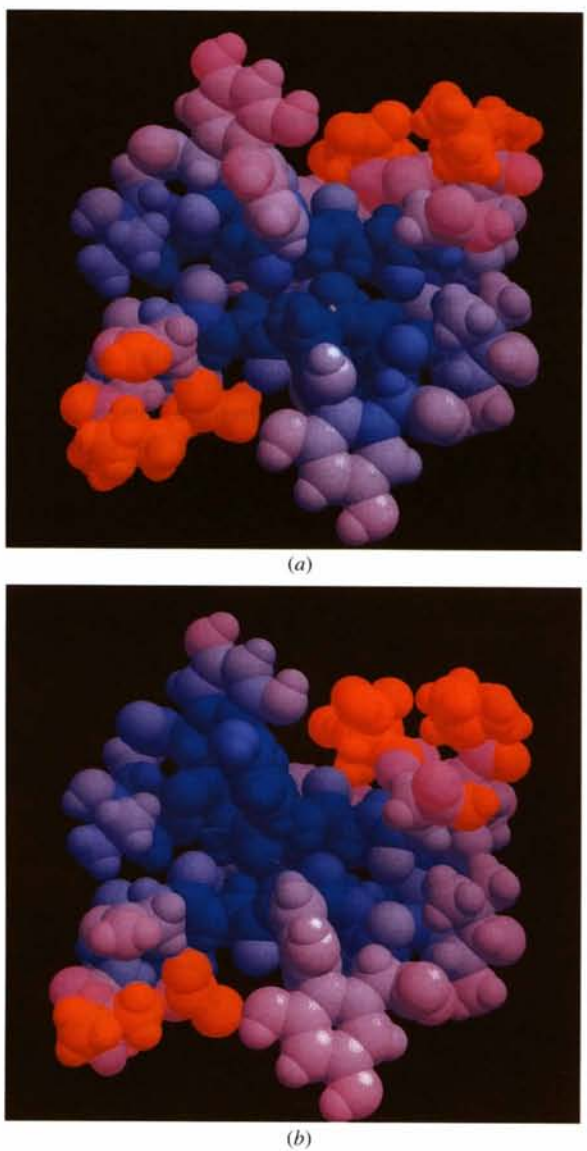

Fig. 8. (*a*)–(*b*) Thermal space-filling model of one balhimycin dimer showing the complexed citrate and acetate ions. The most mobile atoms are shown in red, the least mobile in blue.

molecules, two citrate ions, three acetate ions, three 2-methyl-2,4-pentanediol molecules and 127.5 water molecules in the asymmetric unit in the monoclinic space group $P2_1$. The three-dimensional structure with the numbering scheme of monomer 1 is shown in Fig. 4. Stereoviews of the four independent monomers with 50% probability atomic displacement ellipsoids are shown in Fig. 5. All bond lengths and angles are in the expected range (Engh & Huber, 1991). All four monomers have fairly similar conformations, which is shown by the least-squares fit in Fig. 6. The r.m.s. deviation of the fitted atoms (all non-H atoms except the two glucose residues) was 0.7 Å.

The monomer units are linked together in two different ways. Firstly, the backbone of molecules 1 and 2 form an antiparallel arrangement linked by four amide···carbonyl hydrogen bonds, flanked by antiparallel hydrogen bonds between the N atom in each vancosamine residue and a carbonyl O of the peptide backbone (Fig. 7). One extra hydrogen bond is formed by two hydroxyl atoms of the glucose residues, as proposed by Sheldrick *et al.* (1995). In the ureido-balhimycin dimer the N atom of the vancosamine residue is unable to take part in such hydrogen bonds. Molecules 3 and 4 combine in the same way to constitute the second dimer. Each dimer unit possesses a pseudo-twofold axis, which is however strongly violated by the glucose residues. Secondly, the different dimer units are linked together by two antiparallel hydrogen bonds between two hydroxyl groups of the glucose residues and the O atoms of the keto-hydrate of the vancosamine (molecules 2 and 3, molecule 4 and molecule 1 of the next asymmetric unit) and a hydroxyl group of the glucose residue and a carbonyl O atom of the peptide backbone (molecules 1 and 4, and molecules 3 and 2 of the next asymmetric unit) leading to a chain of connected dimer units. Thus, the aromatic ring systems containing Cl12 and Cl42 are in close contact with one another. The ring systems are fairly parallel to each other with an angle of 9.8° between their best planes, and the two Cl atoms are separated by only 3.63 Å. The monomer units of molecules 1 and 4, and molecules 2 and 3 are also related by pseudo-twofold axes, but these are again strongly violated by the mobile residues and the Cl atoms. All inter- and intramolecular hydrogen bonds involving atoms of the antibiotic molecules are given in Table 3.

All four binding pockets are occupied by solute molecules. In each dimer unit one binding pocket is occupied by a citrate ion, the other by an acetate ion. The carboxyl group of the acetate ion and one carboxyl group of the citrate ion form three strong hydrogen bonds (Fig. 7) to the peptide backbone of the antibiotic molecule. This mimics the binding of the D-Ala-D-Ala terminus of cell-wall peptide. A citrate ion possesses three carboxyl groups that can form hydrogen bonds to the antibiotic peptide. In dimer unit *A*, the carboxyl group attached to a terminal C atom of the citrate ion is bound to the antibiotic, whereas in dimer unit *B* the carboxyl group of the central C atom of the citrate ion forms the hydrogen bonds to the balhimycin molecule. The intermolecular hydrogen-bond geometry to solvent molecules in the binding pocket is given in Table 4.

As seen in Fig. 5 most parts of the molecule are rigid, whereas the glucose and vancosamine residues, and especially the region around the binding pocket, are more flexible. This is also shown in the space-filling model (Fig. 8) where the binding pockets are occupied by either a citrate ion or an acetate ion. This observation supports the idea that the asparagine side chain acts as a 'flap' of the binding pocket as observed in the vancomycin structure (Schäfer, Schneider *et al.*, 1996; Loll *et al.*, 1997), and would move to let the substrate molecules in

Table 3. *Inter- and intramolecular hydrogen-bond geometry between antibiotic molecules*

Hydrogen bonds with $H\cdots A < r(A) + 1.800$ Å and $\angle DHA > 115.0°$.

D—H	*d*(H···*A*)	∠(*D*—H···*A*)	*d*(*D*···*A*)	*A*
N104—H10B	2.01	164.1	2.87	O208
N105—H105	2.14	168.3	3.01	O206
N108—H10G	2.45	125.8	3.05	N102
N108—H10G	2.46	170.8	3.33	O105
N109—H10H	2.04	146.0	2.84	O317^{i}
N109—H10J	2.02	156.3	2.87	O205
O116—H11B	2.14	167.3	2.97	O405
O116—H11B	2.67	114.6	3.12	N309
O117—H11C	1.98	168.4	2.81	O103
O118—H118	2.16	142.8	2.87	O215
O122—H12A	2.20	117.6	2.69	O416^{i}
O123—H123	1.94	158.9	2.74	O417^{i}
N204—H20B	1.98	163.3	2.84	O108
N205—H205	2.18	160.6	3.02	O106
N208—H20F	2.58	120.5	3.12	O424^{ii}
N208—H20G	2.23	161.4	3.08	O410^{ii}
N209—H20H	1.81	163.8	2.69	O105
O215—H215	2.42	172.9	3.26	O114
O216—H21B	2.00	158.6	2.80	O322
O217—H21C	2.65	146.5	3.38	O322
O223—H223	2.64	139.1	3.32	O415
N304—H30B	2.01	162.3	2.86	O408
N305—H305	2.17	163.1	3.02	O306
N308—H30G	2.37	125.4	2.97	N302
N308—H30G	2.43	171.6	3.30	O305
N309—H30H	2.11	138.8	2.85	O117
N309—H30J	2.02	162.7	2.90	O405
O316—H31B	2.27	165.5	3.09	O205^{iii}
O316—H31B	2.60	117.1	3.07	N109^{iii}
O317—H31C	1.95	171.6	2.79	O303
O322—H32A	2.30	118.2	2.80	O216
O323—H323	1.96	177.1	2.80	O217
N404—H40B	2.00	161.4	2.85	O308
N405—H405	2.18	161.5	3.03	O306
N408—H40G	2.24	157.8	3.08	O210^{iv}
N409—H40H	1.83	150.1	2.66	O305
O415—H415	2.06	138.0	2.74	O318
O418—H418	1.90	163.2	2.71	O223
O423—H423	1.95	152.2	2.72	O218^{iii}

Symmetry codes: (i) = $x, y, z + 1$; (ii) = $-x, y + \frac{1}{2}, -z$; (iii) = $x, y, z - 1$; (iv) = $-x, y - \frac{1}{2}, -z$.

Table 4. *Hydrogen-bond geometry between antibiotic molecules and solvent molecules in the binding pocket*

Hydrogen bonds with H···A < $r(A)$ + 1.800 Å and ∠ DHA > 115.0°.

D—H	d(H···A)	∠ (D—H···A)	d(D···A)	A
Molecule 1				
N101—H101	1.97	164.0	2.82	O22C
N102—H102	1.98	151.0	2.78	O21C
N103—H10A	1.96	165.2	2.82	O21C
Molecule 2				
N201—H201	2.04	161.5	2.87	OI2X
N202—H202	2.03	153.3	2.84	OI1X
N203—H20A	2.02	166.9	2.88	OI1X
Molecule 3				
N301—H301	1.93	164.0	2.79	O15C
N302—H302	1.98	148.8	2.77	O16C
N303—H30A	1.99	163.9	2.84	O16C
Molecule 4				
N401—H401	2.03	162.0	2.88	O21X^{i}
N402—H402	2.01	149.1	2.80	O22X^{i}
N403—H40A	1.91	168.6	2.78	O22X^{i}

Symmetry code: (i) = $x-1$, y, z

Table 5. *Hydrogen bonds between antibiotic molecules and solvent molecules*

Hydrogen bonds with H···A < $r(A)$ + 1.800 Å and ∠ DHA > 115.0°.

D—H	d(H···A)	∠ (D—H···A)	d(D···A)	A
N106—H10C	2.07	157.7	2.90	O20S
N107—H10E	1.90	136.0	2.64	O74S^{i}
N108—H10F	1.85	130.9	2.51	O73S
N109—H10I	1.98	159.7	2.86	O35S
N109—H10I	2.44	138.6	3.18	O11H^{ii}
O104—H10K	2.11	138.0	2.79	O46S
O110—H110	1.79	116.8	2.30	O29S
O110—H110	2.07	156.7	2.86	O7S
O111—H11A	1.81	163.3	2.62	O23S
O112—H112	1.91	149.6	2.67	O36S
O115—H115	2.41	125.7	2.98	O18H
O122—H12A	2.40	157.6	3.20	O35S
N206—H20C	2.40	142.7	3.14	O31M
N207—H20D	2.08	148.2	2.91	O3H
N207—H20E	1.76	166.2	2.66	O79S
N209—H20I	2.05	141.9	2.82	O28S
N209—H20J	1.98	158.3	2.85	O50S
O204—H20K	1.85	150.1	2.61	O62S
O210—H210	1.87	156.1	2.66	O8S
O211—H21A	1.82	163.6	2.64	O31S
O212—H212	1.91	157.0	2.70	O9S^{iii}
O218—H218	1.95	162.3	2.76	O5S
O222—H22A	1.93	139.7	2.63	O26S
O223—H223	2.37	134.8	3.02	O18S
N306—H30C	2.04	155.6	2.86	O17S
N307—H30D	2.03	151.4	2.87	O37H^{iv}
N308—H30F	2.09	141.5	2.86	O91S^{iv}
N308—H30F	2.01	123.5	2.68	O26H
N309—H30I	1.99	154.5	2.84	O41S
O304—H30K	2.21	135.4	2.87	O47S
O310—H310	1.86	155.2	2.65	O1S
O311—H31A	1.90	162.7	2.71	O9S
O312—H312	1.92	163.8	2.73	O84S
O315—H315	1.82	173.1	2.65	O8H
O318—H318	1.80	177.4	2.64	O39S
O322—H32A	2.35	160.8	3.16	O41S
N406—H40C	2.04	156.0	2.87	O30S
N409—H40I	2.04	139.8	2.76	O34S
N409—H40J	1.97	152.5	2.81	O80S
O404—H40K	2.22	146.4	2.95	O46S
O410—H410	2.01	156.7	2.80	O16S
O411—H41A	1.92	148.2	2.67	O36S^{v}
O412—H412	1.95	165.6	2.77	O27S^{v}
O416—H41B	2.25	142.7	2.97	O35S^{vi}
O417—H41C	1.85	176.3	2.69	O49S
O422—H42A	1.89	143.2	2.61	O45S
O21M—H21M	1.96	171.2	2.80	O321
O31M—H31M	2.45	140.3	3.14	N206
O17C—H17C	2.39	162.3	3.20	O307

Symmetry codes: (i) = $x-1$, y, z; (ii) = $x+1$, y, $z+1$; (iii) = $-x+1$, $y+\frac{1}{2}$, $-z$ (iv) = $-x$, $y-\frac{1}{2}$, $-z$; (v) = $-x-1$, $y-\frac{1}{2}$, $-z$; (vi) = x, y, $z-1$.

and out. In vancomycin, only one binding pocket is occupied by an acetate ion whereas the remaining one is closed by the asparagine side chain, this second binding pocket is held in a suitable conformation for docking of other molecules or ions.

All other atoms in balhimycin that could take part in hydrogen bonding are on the surface of the molecule and take part in interactions with the remaining solvent. Only one H atom of the protonated secondary amine (N107, N307 and N407) and one H atom of the asparagine side chain (N408) do not appear to form hydrogen bonds to solvent molecules. The hydrogen-bond distances and angles of antibiotic molecules to solvent molecules are given in Table 5.

At a pH of about 7 all the carboxyl groups of the acetate (pK_a = 4.75) and citrate ions [pK_{a1} = 3.14, pK_{a2} = 4.77, pK_{a3} = 6.39 (*Handbook of Chemistry and Physics*, 1987)] should be in the ionic form, leading to a net negative charge. Although some of the H atoms of the vancosamine and methylamine groups (pK_a ≃ 10.7 for the conjugated acids) in each antibiotic molecule do not form hydrogen bonds to solvent molecules, these amines were all refined in the protonated form that should predominate at neutral pH. Thus, each antibiotic molecule has a charge of +1. For overall electrical neutrality there must be five ammonium ions or protonated water molecules in the asymmetric unit. The final difference density did not suggest the presence of other cations such as Na^+.

The authors thank Ludger Häming, Isabel Usón, Ehmke Pohl, Victor Lamzin, Zbigniew Dauter, Keith Wilson, Erich Paulus and Bob Cudney for discussion and encouragment, and to one of the referees for very percipient comments. TRS thanks EMBL for a Predoctoral Fellowship. We thank the Fonds der Chemischen Industrie for support.†

† Atomic coordinates and structure factors have been deposited with the IUCr. Free copies may be obtained through The Managing Editor, International Union of Crystallography, 5 Abbey Square, Chester CH1 2HU, England (Reference: LI0249).

References

Arthur, M. & Courvalin, P. (1993). *Antimicrob. Agents Chemother.* **37**, 1563–1571.

Barna, J. C. J. & Williams, D. H. (1984). *Annu. Rev. Microbiol.* **38**, 339–357.

Beauregard, D. A., Williams, D. H., Gwynn, M. N. & Knowles, D. J. C. (1995). *Antimicrob. Agents Chemother.* **39**, 781–785.

Bernardinelli, G. & Flack, H. D. (1985). *Acta Cryst.* **41**, 500–511.

Brant, M., Wingert, P. & Hager, P. (1994). *Newsweek*, **123**, 38–43.

Chatterjee, S., Vijayakumar, E. K. S., Nadkarni, S. R., Patel, M. V., Blumbach, J., Ganguli, B. N., Fehlhaber, H.-W., Kogler, H. & Vértersy, L. (1994). *J. Org. Chem.* **59**, 3480-3484

Cunha, B. A. (1995). *Antimicrob. Therapy*, **79**, 817–831.

Engh, R. A. & Huber, R. (1991). *Acta Cryst.* A**47**, 392–400.

Flack, H. D. (1983). *Acta Cryst.* A**39**, 876–881.

Fujinaga, M. & Read, R. J. (1987). *J. Appl. Cryst.* **20**, 517–521.

Garman, E. & Schneider, T. R. (1997). *J. Appl. Cryst.* **30**, 211–237.

Gerhard, U., MacKay, J. P., Maplestone, R. A. & Williams, D. H. (1993). *J. Am. Chem. Soc.* **115**, 232–237.

Groves, P., Searle, M. S., MacKay, J. P. & Williams, D. H. (1994). *Structure*, **2**, 747–754.

Handbook of Chemistry and Physics (1987). Edited by R. C. Weast, M. J. Astle & W. H. Beyer, 68th ed., p. D163. Ohio: The Chemical Rubber Co.

Harris, C. M., Kopecka, H. & Harris, T. M. (1983). *J. Am. Chem. Soc.* **105**, 6915–6922.

Hirschfeld, F. L. (1976). *Acta Cryst.* A**32**, 239-244.

Levine, J. F. (1987). *Med. Clin. North. Am.* **71**, 1135-1145.

Loll, P., Bevivino, E., Korty, B. D. & Axelsen, P. H. (1997). *J. Am. Chem. Soc.* **119**, 1516–1522.

MacKay, J. P., Gerhard, U., Beauregard, D. A., Westwell, M. S., Searle, M. S. & Williams, D. H. (1994). *J. Am. Chem. Soc.* **116**, 4581–4590.

Miller, R., DeTitta, G. T., Jones, R., Langs, D. A., Weeks, C. M. & Hauptman, H. A. (1993). *Science*, **259**, 1430–1433.

Miller, R., Gallo, S. M., Khalak, H. G. & Weeks, C. M. (1994). *J. Appl. Cryst.* **27**, 613–621.

Nadkarni, S. R., Patel, M. V., Chatterjee, S., Vijayakumar, E. K. S., Desikan, K. R., Blumbach, J. & Ganguli, B. N. (1994). *J. Antibiot.* **47**, 334–341.

Navaza, J. (1994). *Acta Cryst.* A**50**, 157–163.

Navaza, J. & Vernoslova, E. (1995). *Acta Cryst.* A**51**, 445–449.

Neu, H. C. (1992). *Science*, **257**, 1064–1073.

Otwinowski, Z. & Minor, W. (1996). *HKL: program system for macromolecular data processing*. Southwestern Medical Center, University of Texas, Dallas, USA, and University of Virginia, Charlottesville, USA.

Pearce, C. M., Gerhard, U. & Williams, D. H. (1995). *J. Chem. Soc. Perkin Trans. II*, pp. 159–162.

Pearce, C. M. & Williams, D. H. (1995). *J. Chem. Soc. Perkin Trans. II*, pp. 153–158.

Polk, R. E., Israel, D., Wang, J., Lenitz, J., Miller, J. & Stotka, J. (1993). *Antimirob. Agents Chemother.* **37**, 2139–2143.

Prowse, W. G., Kline, A. D., Skelton, M. A. & Loncharich, J. (1995). *Biochemistry*, **34**, 9632–9644.

Rademacher, P. (1987). *Strukturen Organischer Moleküle*, 1st ed. New York: VCH.

Reynolds, P. E. (1989). *Eur. J. Microb. Infect. Dis.* **8**, 943–950.

Rogers, D. W. (1994). *Structure*, **2**, 1135–1140.

Rollet, J. S. (1970). *Crystallographic Computing*, edited by F. R. Ahmed, S. R. Hall & C. P. Huber, pp. 167–181. Copenhagen: Munksgaard.

Schäfer, M., Pohl, E., Schmidt-Bäse, K., Sheldrick, G. M., Hermann, R., Malabarba, A., Nebuloni, M. & Pelizzi, G. (1996). *Helv. Chim. Acta*, **79**, 1916–1924.

Schäfer, M., Schneider, T. R. & Sheldrick, G. M. (1996). *Structure*, **4**, 1509–1515.

Sheldrick, G. M. (1990). *Acta Cryst.* A**46**, 467–473.

Sheldrick, G. M., Dauter, Z., Wilson, K. S., Hope, H. & Sieker, L. C. (1993). *Acta Cryst.* D**49**, 18–23.

Sheldrick, G. M. & Gould, R. O. (1995). *Acta Cryst.* B**51**, 423–431.

Sheldrick, G. M., Jones, P. G., Kennard, O., Williams, D. H. & Smith, G. A. (1978). *Nature (London)*, **271**, 223–225.

Sheldrick, G. M., Paulus, E., Vértesy, L. & Hahn, F. (1995). *Acta Cryst.* B**51**, 89–98.

Sheldrick, G. M. & Schneider, T. R. (1997). *Methods Enzymol.* **277**, 319–343.

Teng, T.-Y. (1990). *J. Appl. Cryst.* **23**, 387–391.

Trueblood, K. N. & Dunitz, J. P. (1983). *Acta Cryst.* B**39**, 6014–6018.

Vértesy, L., Fehlhaber, H.-W., Kogler, H. & Limbert, M. (1996). *J. Antibiot.* **49**, 115–118.

Waitho, J. P. & Williams, D. H. (1989). *J. Am. Chem. Soc.* **111**, 2475–2480.

Walsh, C. T. (1993). *Science*, **261**, 308–309.

Walsh, C. T., Fisher, S. I., Park, I.-S., Prahalad, M. & Wu, Z. (1996). *Chem. Biol.* **3**, 21-28.